Barrier Properties of Polyhydroxybutyrate/Ethyl Cellulose-blend-coated Paper through the Incorporation of Organo-modified Nanoclay as a Coating Component

Yong Ju Lee,[a] Dong Gun Lim,[a] Ji Eun Cha,[a] Do Young Lee,[a] Tai-Ju Lee,[b,*] and Hyoung Jin Kim [a,*]

A sodium bentonite product (nanoclay) was added to a polyhydroxybutyrate/ ethyl cellulose (PHB/EC) blend coating agent, and the impact of the nanoclay content on the properties of the coated paper was investigated. The organically treated nanoclay exhibited enhanced compatibility with the PHB/EC blend, ensuring uniform dispersion within the coating layer and improving the barrier properties of the coated paper. The mechanical properties of the PHB/EC blend-coated paper with nanoclay demonstrated ductile behavior, reducing the tensile strength and increasing the elongation. However, at higher nanoclay loadings, specifically up to 25%, aggregation among nanoclay particles occurred. This hindered the enhancement of barrier properties, thereby decreasing the degree of elongation. Incorporating nanoclay as a filler in the PHB/EC blend at suitable levels showed potential for further enhancing the barrier properties and ensuring economic feasibility in the production of packaging paper.

DOI: 10.15376/biores.19.3.4782-4799

Keywords: Polyhydroxybutyrate; Ethyl cellulose; Nanoclay; Nano-organo bentonite; Organo-modification; Biodegradable polymers; Barrier coating

*Contact information: a: Department of Forest Products and Biotechnology, Kookmin University, 77 Jeongneung-ro, Seongbuk-gu, Seoul 02707 Republic of Korea; b: National Institute of Forest Science, Department of Forest Products and Industry, Division of Forest Industrial Materials, 02455, Seoul, Republic of Korea; *Corresponding authors: leetj@korea.kr; hyjikim@kookmin.ac.kr*

INTRODUCTION

With the rapid emergence of environmental pollution issues caused by plastic wastes (Geyer *et al.* 2017), the European Union (EU) has published the legislation EU/2018/852 as a part of its efforts to promote the recycling of packaging waste as a component of establishing a circular economy system (2018). In addition, within the Republic of Korea, comprehensive measures for the management of recyclable waste to reduce plastic waste have been implemented (2018). As regulations on packaging waste disposal become more stringent, there is a growing focus on biodegradable polymers as alternatives to non-biodegradable petroleum-based polymers in the field of paper packaging, such as paper-based packaging. However, due to the porous structure of paper and the hydrophilicity of hydroxyl groups present in the main component cellulose molecules, paper exhibits low resistance to moisture. Therefore, barrier coating treatment is required to impart hydrophobicity (Khwaldia *et al.* 2010).

Polyhydroxyalkanoates (PHAs) are bio-based biodegradable polymers that accumulate in granular form during microbial cultivation during an imbalanced nutrient

supply, thus serving as internal energy storage. The monomeric units forming PHAs exceed 150 types, enabling the diversification of properties such as structure and molecular weight by adjusting substrate and strain selection, as well as microbial cultivation conditions (Verliden *et al.* 2007; Bedian *et al.* 2017).

The degradation of PHAs has been confirmed not only under anaerobic conditions such as methane fermentation processes but also in facultative anaerobic marine environments (Wang *et al.* 2018). In contrast to polylactic acid (PLA), a representative biodegradable plastic that decomposes only under specific composting conditions, the use of PHAs, known for their excellent biodegradability, is considered more environmentally friendly. Given the challenges posed by the limited composting conditions for PLA (Ko *et al.* 2021), the application of PHAs is expected to contribute to the reduction of microplastics (Cole *et al.* 2011), which is a serious environmental concern, particularly in marine ecosystems.

Poly(3-hydroxybutyrate) (PHB) is the most widely produced form among polyhydroxyalkanoates (PHAs) (Aramvash *et al.* 2015) and it exhibits mechanical properties comparable to those of general-purpose plastics such as polypropylene (PP) (Harding *et al.* 2007). It possesses excellent blocking resistance due to its high crystallinity and hydrophobic nature (Seoane *et al.* 2017). In addition, the 3-hydroxybutyrate (3HB) oligomers constituting PHB demonstrate outstanding biocompatibility, being found within the human body (Koller *et al.* 2010). Based on these characteristics, PHB has found applications in the field of food and pharmaceutical packaging, with ongoing research exploring its use as a coating material for paper (Bugnicourt *et al.* 2014; Khosravi-Darani and Bucci 2015). Cyras *et al.* (2007; 2009) performed to enhance the barrier properties of paper and reduce PHB consumption by manufacturing biodegradable composite films using PHB and paper. Similarly, Safari and van de Ven (2015) investigated the impact of PHB crystallization conditions on the mechanical and barrier properties of coated paper, demonstrating the feasibility of using PHB as a coating material for paper. However, challenges such as high production costs and suboptimal properties compared with conventional polymers hinder its commercialization. To address these challenges, the application of alternative polymers and additives is required (Bugnicourt *et al.* 2014).

In this regard, there have been attempts to manufacture coatings by adding cellulose to PHB. Rastogi and Samyn (2017; 2020) produced a superhydrophobic coating using nanofibrillated cellulose (NFC) as a binder for PHB nanoparticles, while improving the properties of the coating by blending hydrophobically modified microfibrillated cellulose with PHB. Additionally, Seoane *et al.* (2018a,b) enhanced the interfacial bonding and properties between PHB and paper using cellulose nanocrystals (CNC).

Cellulose, a renewable material, can be chemically modified to produce cellulose derivatives with various properties (Liu *et al.* 2021). Among these derivatives, ethyl cellulose (EC), which is hydrophobic and thermally stable, is used as a coating material in various industries because of its excellent mechanical properties, film-forming ability, biodegradability, and nontoxic nature (Li *et al.* 2015; Heinze *et al.* 2018; Ahmadi *et al.* 2020). Research has been conducted on blending EC with poly(3-hydroxybutyrate) (PHB) to manufacture blends, and previous studies have performed analyses on the structure, crystallization behavior, mechanical properties, and applications as a biomedical material of PHB/EC blends (Zhang *et al.* 1997; Finelli *et al.* 1998; Chan *et al.* 2011; Costa *et al.* 2013; Chen *et al.* 2016; Lim *et al.* 2024).

Using nanocomposites and employing nanosized fillers such as clay to enhance the properties of polymer blends is an effective method. When applied to paper coatings,

nanocomposites can improve mechanical and barrier properties and offer the advantage of reducing the amount of polymer material used, thereby ensuring economic viability (Gaikwad *et al.* 2015). However, research incorporating nanoclay as a filler for PHB/EC blend coatings has not been reported to date, and studies evaluating the potential use of these coatings as packaging materials for paper are lacking. In this study, the effect of incorporating nanoclay as a filler for PHB/EC blend coating on the barrier properties of paper substrates was investigated.

EXPERIMENTAL

Materials

Base paper

Table 1 shows the base paper used for coating and its basis weight, thickness, apparent density, and roughness. The basis weight, thickness, and apparent density were determined according to ISO 534. The surface roughness of the base paper was measured using OptiTopo surface deviation (OSD) equipment (L&W, Sweden).

Table 1. Physical Properties of the Base Paper

Properties	Value
Basis weight (g/m^2)	58.8 ± 0.2
Thickness (μm)	59.4 ± 0.9
Apparent density (g/cm^3)	0.990 ± 0.008
Roughness (OSD) (μm)	0.639 ± 0.002

Coating polymers

For the coating of the base paper, the biodegradable polymer used was poly(3-hydroxybutyrate) (PHB) pellets (molecular weight: 550,000 g/mol, nominal granule size: 5 mm) from Goodfellow Co., Ltd. As a cellulose derivative for manufacturing polymer blends, ethyl cellulose (EC, 48.0% to 49.5% ethoxy) powder from Sigma-Aldrich Co., Ltd. was used. The comparative group used polylactic acid (PLA, 2002D) pellets of extrusion sheet grade from NatureWorks Co., Ltd.

Filler for coating polymers

The nanoclay used as a filler for the coating polymer was sodium bentonite clay from Alfa Aesar Co., Ltd. The cation exchange capacity (CEC) of the bentonite clay was 78 meq/100g, and the pass-through fraction was sieved through a 325-mesh screen.

Methods

Preparation of organo nanoclay

Ensuring uniform dispersion of clay within the polymer matrix is a crucial factor in enhancing the barrier properties of polymer/clay nanocomposites. However, due to the platelet-like structure and hydrophilic surface of clay, aggregation occurs within organic polymers, making uniform dispersion challenging. To address this issue, surface modification of clay is required to enhance its compatibility with polymers (Fatyeyeva *et al.* 2017).

Clay platelets can be organophilized by replacing the Na^+ and Ca^{2+} ions present

between the layers with organic cations such as alkylammonium through cation exchange reactions. Organophilized clay exhibits improved compatibility with organic polymers and increased interlayer spacing between each platelet layer (Cui *et al.* 2015; Fatyeyeva *et al.* 2017).

The mechanism underlying the enhancement of barrier properties in polymer/clay nanocomposites is attributed to the formation of a tortuous path, as illustrated in Fig. S1, whereby clay nanoparticles are uniformly dispersed within the polymer matrix. In cases where clay is absent within the polymer, gas or water molecules may travel the shortest distance (*d*). However, when impermeable clay is dispersed, the actual distance (*d*') increases, thereby delaying diffusion through the polymer matrix. The barrier properties are influenced by the aspect ratio (*L*/*W* ratio) of the clay and the degree of exfoliation and dispersion of clay platelets (Gaikwad *et al.* 2015; Fatyeyeva *et al.* 2017).

To enhance compatibility with poly(3-hydroxybutyrate)/ethyl cellulose (PHB/EC) blends, organically modified nanoclay was synthesized by introducing octadecylamine (ODA) between the silicate layers of bentonite clay through a cation exchange interaction. The procedure followed previously reported methods (Agag and Takeichi 2000; Motawie *et al.* 2014). The quantity (g) of the organic modifier ODA used for the organophilic treatment of bentonite clay was calculated as follows,

$$X = \frac{78}{100} \times A \times 1.3 \times \frac{MW}{1000} \quad (1)$$

where *A* is the quantity of bentonite clay for the reaction, MW is the molecular weight (269.509 g/mol) of ODA, 78/100 is the CEC of bentonite clay, and 1.3 signifies 30% excess of the organic modifier (ODA) relative to the CEC of bentonite clay. The factor 1000 is used for unit conversion.

To convert the calculated amount of ODA into a form suitable for a cation exchange reaction, hydrochloric acid (HCl) was added at a 1:1 equivalent ratio. The resulting octadecylamine hydrochloride solution was prepared by completely dissolving the treated ODA in distilled water at 80 °C at a concentration of 1%. Bentonite clay was swollen using distilled water at 2% concentration with stirring for 3 h at 80 °C to facilitate the penetration of the organic modifier between the layers. The swollen bentonite clay suspension was mixed with the octadecylamine hydrochloride solution, and the process was performed under strong stirring at 80 °C for 12 h. Next, the unreacted materials were removed by repeated washing with distilled water and ethanol at 80 °C. The washed nanoclay was then dried at 105 °C and ground, and the fraction passing through a 325-mesh sieve was collected.

The crystal structure of the prepared nanoclay and confirmation of the structure with ODA inserted between the layers were analyzed using X-ray diffraction (XRD) with Cu-Kα radiation (λ = 1.54 Å) on an X-ray diffractometer (Ultima IV, Rigaku, Japan). The analysis conditions included a 40 kV voltage, 30 mA current, and a scanning rate of 2°/min over the 2θ range of 3 to 10° with a 0.02° interval. Based on the analyzed results, the interlayer distance (d-spacing) of the nanoclay was calculated using Eq. 2 according to Bragg's law.

$$n\lambda = 2d_{001} \sin\theta \quad (2)$$

where *n* is the integer corresponding to the first order of reflection, *d* is the interlayer distance of the crystal plane (001), λ is the wavelength of the incident X-ray (1.54 Å), and θ is half of the peak diffraction angle.

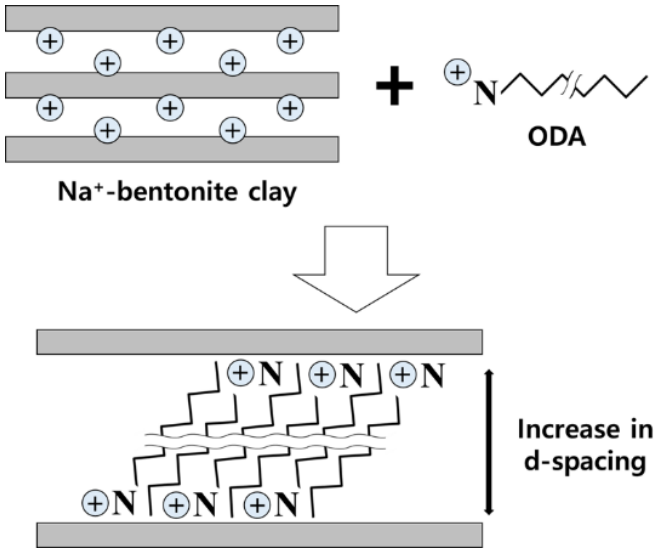

Fig. 1. Schematic presentation of the structure of ODA-intercalated bentonite clay

Coating of the PHB/EC blend with nanoclay on paper

Following recent work (Lim *et al.* 2021; 2024), the coating of papers was performed by adding nanoclay to the PHB/EC coating blend with the most superior barrier properties, which was the 50:50 (w/w) ratio of PHB/EC (hereafter referred to as EC50). The nanoclay content was varied according to the conditions presented in Table 2. After completely dispersing the nanoclay in chloroform through ultrasonication, a coating solution with a concentration of 10 ± 1 wt% was prepared by mixing it with the PHB/EC blend solution. Coating was performed on the base paper using a four-sided applicator and an auto bar coater (Gist, Korea) at a speed of 20 mm/s. The gap size of the applicator was adjusted to control coating weight for 18 ± 1 g/m^2 (Lim *et al.* 2024).

Table 2. Nanoclay Content in PHB/EC Blend for Paper Coating

Sample Code	Nanoclay weight fraction in PHB/EC (EC50) blend (wt%)
EC50_NC5	5
EC50_NC10	10
EC50_NC15	15
EC50_NC20	20
EC50_NC25	25

Morphological analysis

Changes in the morphology of the coating layer with varying nanoclay content were observed using scanning electron microscopy (FE-SEM, JSM-7401F, JEOL, Japan). In addition, to confirm the distribution of nanoclay within the coating layer, energy-dispersive X-ray spectroscopy (EDS, X-Max, Oxford Instruments, UK) was employed for mapping analysis of the major constituent element, Si, in nanoclay specimens.

Barrier properties

To evaluate the barrier properties required for packaging paper, the air permeability, Cobb size degree, water vapor transmission rate, and oil resistance of the PHB/EC blend

coating with nanoclay were analyzed. The air permeability was analyzed according to ISO 5636–3 using an air permeance tester (L&W, Sweden). The Cobb size degree was analyzed following ISO 535, measuring the absorption over 1800 s at room temperature. For the analysis of the water vapor transmission rate (WVTR), the calcium chloride method following KS T 1305 was employed, and measurements were performed at 40 ℃ and 90% relative humidity for more than 24 h. Oil resistance was also evaluated using the Kit test according to the TAPPI method T 559.

Mechanical properties

The tensile strength and strain rate of the papers were analyzed using a tensile tester (L&W, Sweden) according to ISO 1924–3.

RESULTS AND DISCUSSION

Morphologies

Figure 2 shows an SEM photograph of the incorporation of organo-modified nanoclay in PHB/EC blend-coated paper (EC50) at a magnification of 500×. When 5% of unmodified clay (sodium bentonite clay) was added to the PHB/EC blend-coated paper, the clay aggregated on the surface of the coating layer, as shown in Fig. 2a. However, as shown in Fig. 2b–e, as organo-modified nanoclay was mixed in the range of 5 to 20% in the PHB/EC blend, it was observed to be uniformly dispersed in the coating layer without any agglomeration. This is attributed to the introduction of hydrophobic alkyl chains between the layers of nanoclay through organic modification, resulting in increased compatibility with the PHB/EC blend, as evidenced by the XRD analysis shown in Fig. 3. The interlayer distance of the alkyl-chain-modified nanoclay was measured to be 19.12 Å, indicating an increase of 6.55 Å compared with the unmodified clay with an interlayer distance of 12.57. The dispersibility in chloroform, the solvent used for the PHB/EC blend shown in Fig. 4, was evaluated. The hydrophilic untreated clay showed poor dispersion and sedimentation, whereas the nanoclay was completely dispersed in the hydrophobic chloroform. However, when the nanoclay content was increased up to 25%, a structure was formed in which nanoclay aggregated within the PHB/EC blend, as shown in Fig. 2f. Isa *et al.* (2020) found that the addition of organically modified nanoclay to PHB resulted in the occurrence of aggregation with increasing nanoclay content. The result of Fig. 2f corresponds to this.

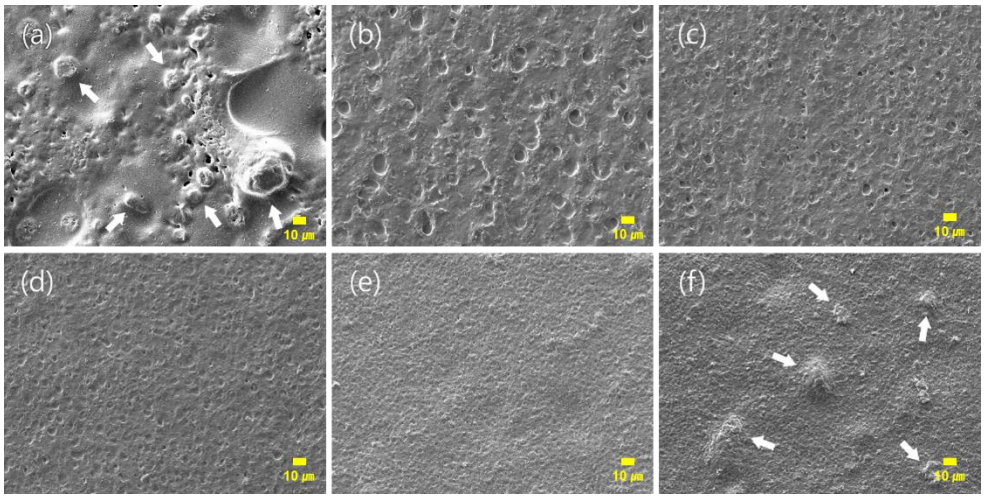

Fig. 2. FE-SEM images (×500) of the PHB/EC blend (EC50) coated paper with nonmodified clay (a: 5 wt%) and modified clay nanoclay (b: 5 wt%, c: 10 wt%, d: 15 wt%, e: 20 wt% and f: 25 wt%)

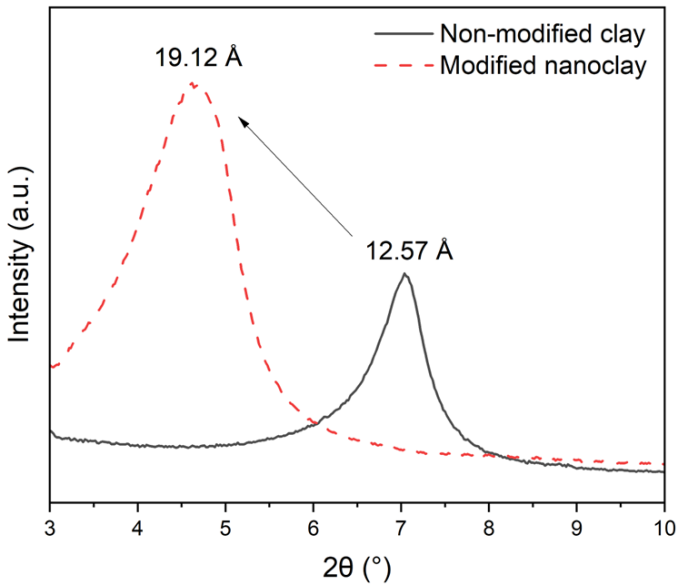

Fig. 3. X-ray diffraction patterns of the nonmodified clay and modified nanoclay

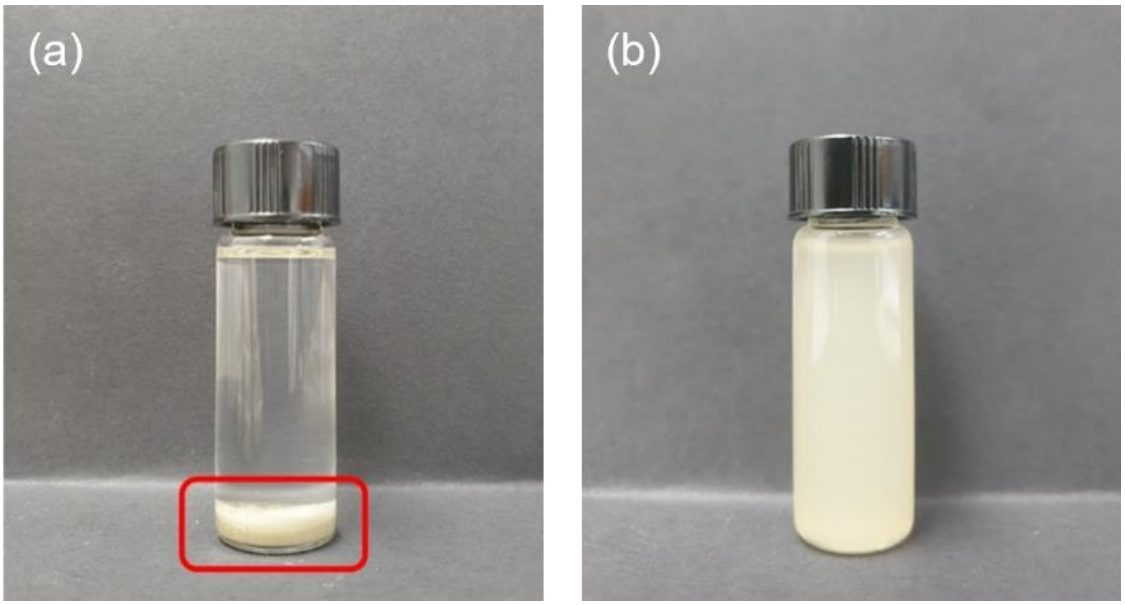

Fig. 4. Dispersibility of nonmodified clay (a) and modified nanoclay (b) in chloroform

Figure 5 shows EDX mapping images of the Si element on the coated paper surface, indicating the distribution of nonmodified clay and nanoclay within the PHB/EC blend coating layer. In Fig. 5a, the nonmodified clay exhibits a pattern corresponding to the results of the scanning electron microscopy analysis, with aggregated Si elements observed randomly. Figures 5b–f show the uniform dispersion of nanoclay, with an increasing nanoclay content leading to an expanded Si distribution area within the coating layer. In addition, the elemental composition ratios on the coating surface are illustrated in Fig. 6, highlighting differences based on clay modification and loading levels. Comparing the elemental composition ratios of nonmodified clay and nanoclay at a 5% loading in Fig. 6a and 6b, nonmodified clay demonstrated a lower Si ratio (0.84%) than organo-modified nanoclay, which measured 1.54%. These results suggest that nanoclay, dispersed uniformly due to organic modification, exhibited a higher specific surface area than agglomerated nonmodified clay in the coating layer. In Figs. 6b–f, an increase in the Si ratio proportional to the nanoclay loading was evident.

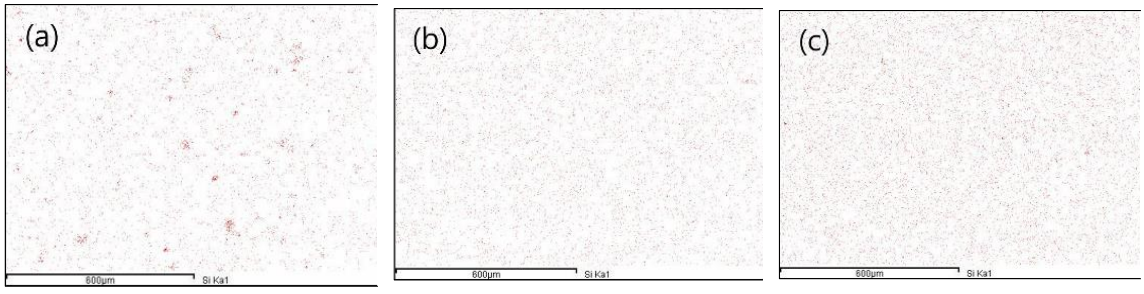

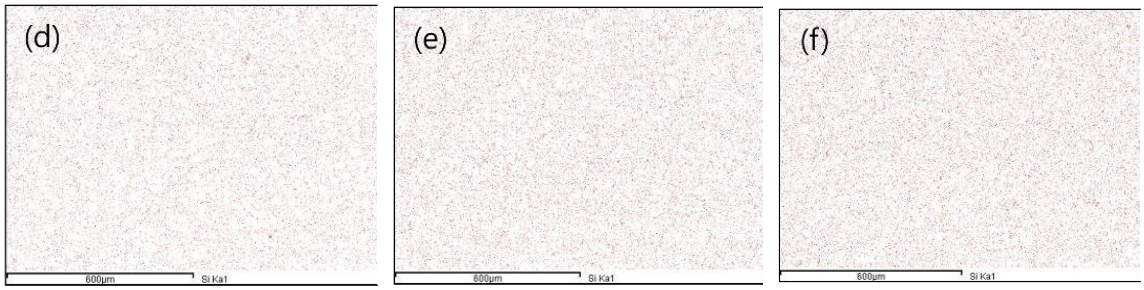

Fig. 5. EDS mapping images of nonmodified clay (a: 5 wt%) and modified nanoclay (b: 5 wt%, c: 10 wt%, d: 15 wt%, e: 20 wt% and f: 25 wt%) distribution in the PHB/EC blend (EC50) coated paper

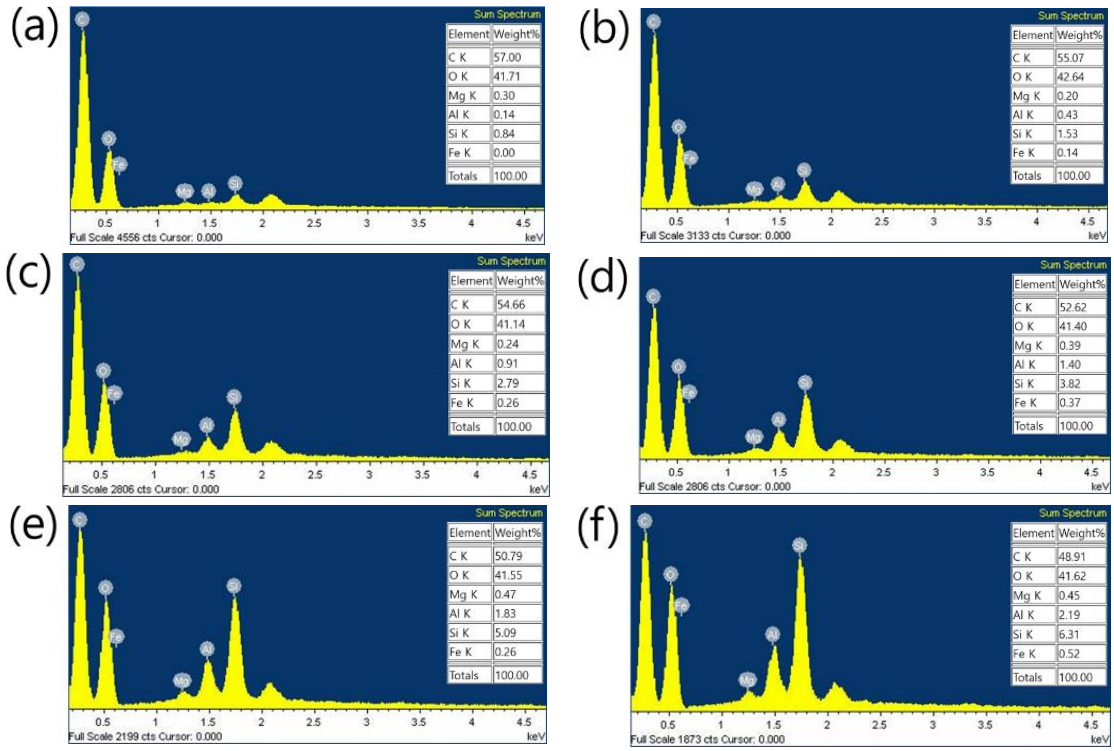

Fig. 6. EDS spectra of the surface of the PHB/EC blend (EC50) coated glassine paper with nonmodified clay (a: 5 wt%) and modified nanoclay (b: 5 wt%, c: 10 wt%, d: 15 wt%, e: 20 wt% and f: 25 wt%)

Figure 7 shows an SEM image of the surface of the PHB/EC blend coating with nanoclay at a magnification of 3,000x. The results show that clay particles at the nanometer scale were exposed on the surface of the coating layer. Furthermore, with an increase in the nanoclay content, the size of the fibril structure formed on the coating layer decreased, and the boundaries became less distinct, indicating improved miscibility between PHB and EC. This suggests that nanoclay acted as a nucleating agent for PHB, leading to the simultaneous formation of more and smaller crystals, enhancing the uniformity of the coating (Botana *et al.* 2010).

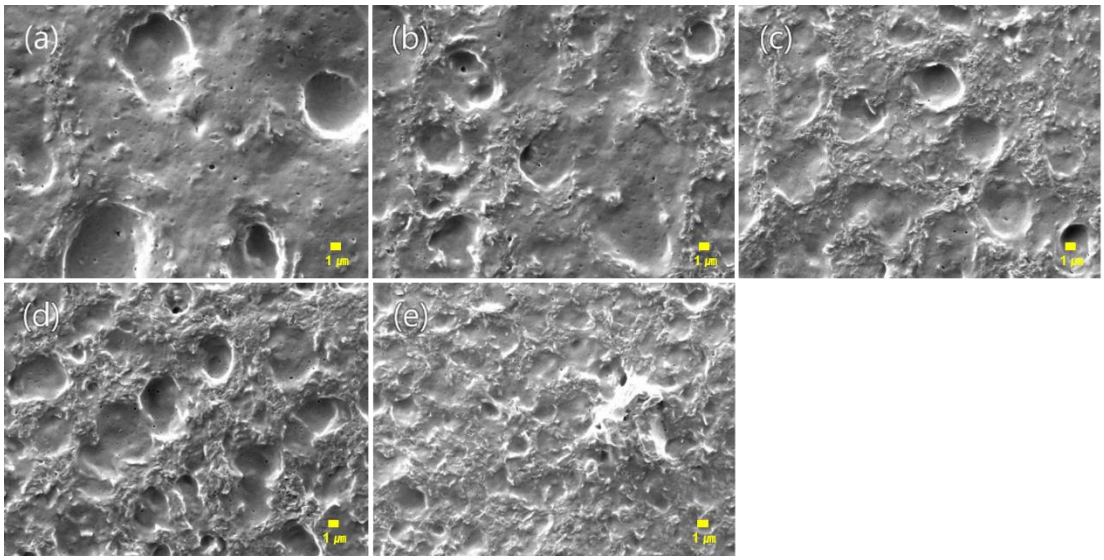

Fig. 7. FE-SEM images (×3000) of the PHB/EC blend (EC50) coated paper with modified nanoclay (a: 5 wt%, b: 10 wt%, c: 15 wt%, d: 20 wt% and e: 25 wt%)

Barrier Properties

Air permeability

Figure 8 shows the changes in air permeability concerning the nanoclay content in the PHB/EC coating blend. For comparative analysis, the air permeability of the PLA- and PHB-coated paper was simultaneously presented. The PLA-coated paper has a minimum value (0.265 mL/min) of air permeability at a coated weight of 18 g/m^2. Furthermore, the PLA-coated paper exhibited higher air permeability than the PHB-coated paper at the same coated weight. The PHB/EC blend-coated paper also showed the lowest air permeability under all conditions, regardless of the nanoclay content. As previously confirmed in the morphological characteristics analysis results, the continuity of the coating layer was maintained as the hydrophobic nanoclay was uniformly distributed within the PHB/EC blend matrix. Despite this, aggregation resulted when the content of nanoclay was increased to 25. Although the ratio of the PHB/EC blend polymer was reduced, it did not affect the coverage of the coating layer.

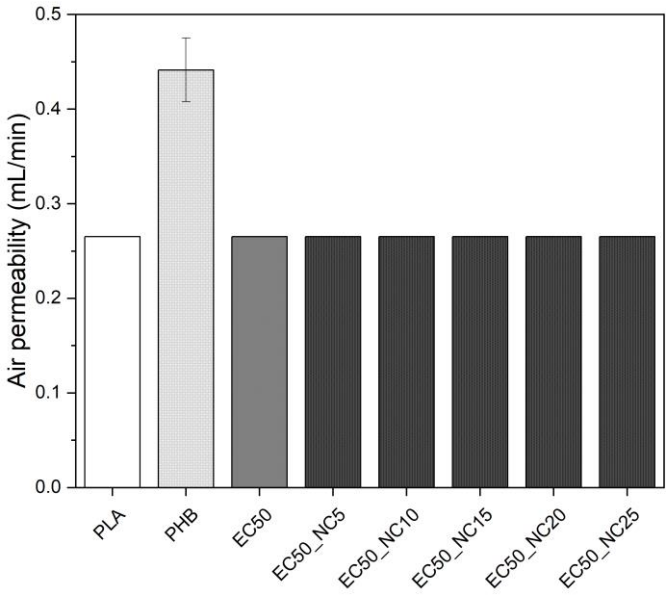

Fig. 8. Changes in air permeability of nanoclay- reinforced PHB/EC blend (EC50) coated paper (coat weight: 18 g/m^2) depending on nanoclay content

Cobb size degree

Figure 9 shows the Cobb size degree (water sorption rate) of the PLA and PHB coatings, along with the variation in WVTR of PHB/EC blend (EC50) coatings with different nanoclay contents. The water sorption of PLA-coated paper was 2.1 g/m^2, which was approximately 8% of the PHB coating level and indicated a relatively superior water resistance. The Cobb size degree of PHB/EC blend coatings gradually decreased with an increase in nanoclay content, demonstrating an improvement in water resistance. The absorption of EC50_NC20, where nanoclay was mixed at a 20% ratio, was 2.2 g/m^2, approximately 27% lower than that of the EC50 condition without nanoclay, showing water resistance at a level similar to that of PLA-coated paper. This is attributed to the enhanced compatibility of PHB and EC due to the addition of nanoclay, which increased the uniformity of the coating layer. The impermeable nanoclay particles form long pathways within the PHB/EC coating, increasing the distance water molecules must traverse to pass through the coating layer and move toward the substrate (Gaikwad *et al.* 2015; Fatyeyeva *et al.* 2017). However, in the case of EC50_NC25 with 25% nanoclay, the sorbed water remained the same as that in EC50_NC20, suggesting diminished additional improvement in water resistance. This is attributed to the aggregation of nanoclay within the PHB/EC blend, inhibiting further enhancement of water resistance in the coated paper.

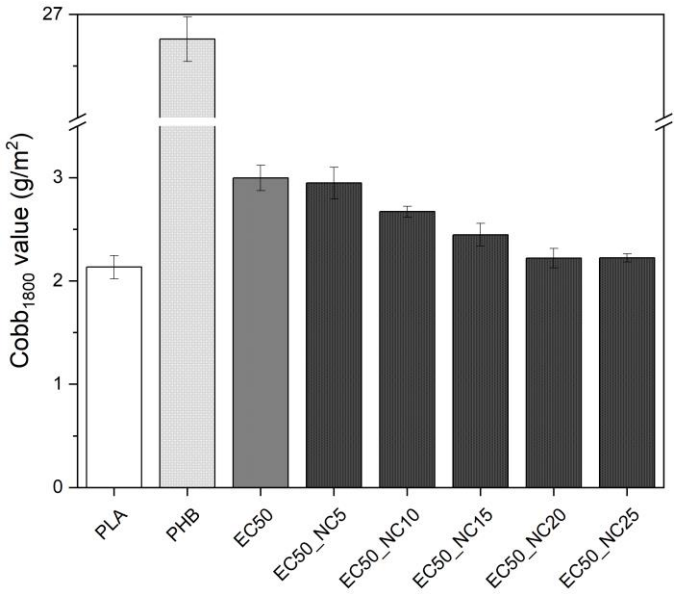

Fig. 9. Changes in the cobb1800 value of the nanoclay- reinforced PHB/EC blend (EC50) coated paper (coat weight: 18 g/m^2) depending on the nanoclay content

Water vapor transmission rate

Figure 10 shows the WVTR measurements of PLA- and PHB-coated papers, along with the changes in WVTR of PHB/EC blend (EC50) coatings with varying nanoclay contents. WVTR results, similar to Cobb size degree measurements, showed that PLA-coated paper exhibited approximately 70% lower WVTR (290.5 g/(m^2·day)) than PHB-coated paper, indicating superior moisture resistance.

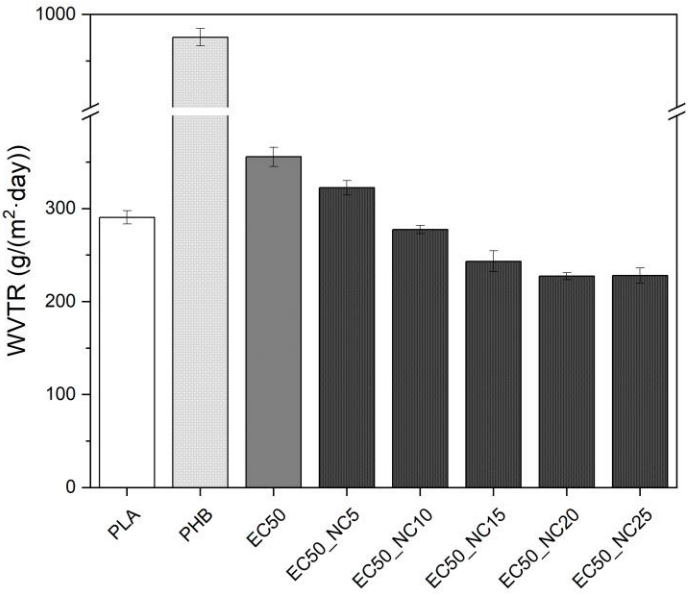

Fig. 10. Changes in the water vapor transmission rate of the nanoclay- reinforced PHB/EC blend (EC50) coated paper (coat weight: 18 g/m^2) depending on the nanoclay content

For PHB/EC blend coatings, increasing the nanoclay content decreased WVTR, resulting in enhanced moisture resistance. The condition with the lowest WVTR was EC50_NC20, showing 227.3 g/(m^2·day), representing an approximately 36% decrease

compared to the EC50 condition and demonstrating superior moisture resistance compared with PLA-coated paper. The WVTR of EC50_NC25 was 228.0 g/(m^2·day), showing a similar trend to the absorption measurement results, with little difference compared to EC50_NC20. These findings suggest that the impermeable nanoclay dispersed within the PHB/EC blend formed long pathways that restricted water vapor diffusion, leading to reduced WVTR. In addition, the increased nanoclay content of up to 25% resulted in aggregation, potentially diminishing the moisture resistance of the coating layer.

Kit test

Figure 11 shows the oil resistance results of the PLA- and PHB-coated paper, along with the changes in the oil resistance of the PHB/EC blend (EC50) coated paper with varying nanoclay contents. The oil resistance of the PLA-coated paper, recorded at the highest rating of 12, surpassed that of the PHB coating with a rating of 5.6, indicating higher grease resistance. The variation in oil resistance of PHB/EC blend-coated paper with different nanoclay contents remained constant at a maximum rating of 12 for all conditions, similar to the results obtained from the oil resistance tests. This further supports the notion that nanoclay, enhanced in compatibility with the PHB/EC blend due to organic modification, maintained a dispersed structure in the coating, creating a condensed layer impervious to oil penetration, and hence a constant grease resistance rating of 12.

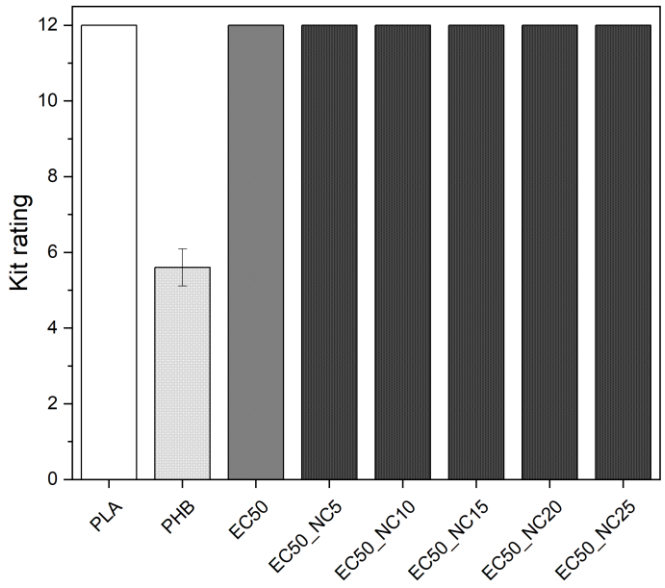

Fig. 11. Changes in the kit rating of nanoclay- reinforced PHB/EC blend (EC50) coated paper (coat weight: 18 g/m^2) depending on nanoclay content.

Mechanical properties

Figure 12 shows the tensile strength and elongation at break results for PLA- and PHB-coated paper, as well as PHB/EC blend (EC50) coatings with varying nanoclay contents. The tensile strength of the PLA and PHB coatings showed a marginal difference of 0.04 kN/m, indicating a comparable level, while the EC50 condition exhibited a slightly higher tensile strength of 6.72 kN/m, approximately 6% higher than that of PLA. In contrast, the elongation at break revealed that the ductile PLA coating had a higher value of 2.30%, surpassing the brittle PHB and EC50 conditions. For the PHB/EC blend coatings with nanoclay, an increasing nanoclay content led to a decreasing trend in tensile strength, with

a slight increase in elongation at break observed under some conditions. The tensile strength of the EC50_NC5 condition was 6.69 kN/m, showing a negligible difference compared with the EC50 condition, while the elongation at break increased by approximately 8%, indicating improved ductility. However, as the nanoclay content increased, both the tensile strength and elongation at break gradually decreased. In the EC50_NC25 condition, these values were approximately 7% and 2% lower, respectively, than those in the EC50 condition. This suggests that the nucleating effect of nanoclay, leading to a smaller crystallite size in PHB, resulted in ductile behavior (Lee *et al.* 1987). Moreover, at the high level of 25% nanoclay, the aggregated clay interfered with the interactions among PHB/EC blend polymers, significantly decreasing the mechanical properties.

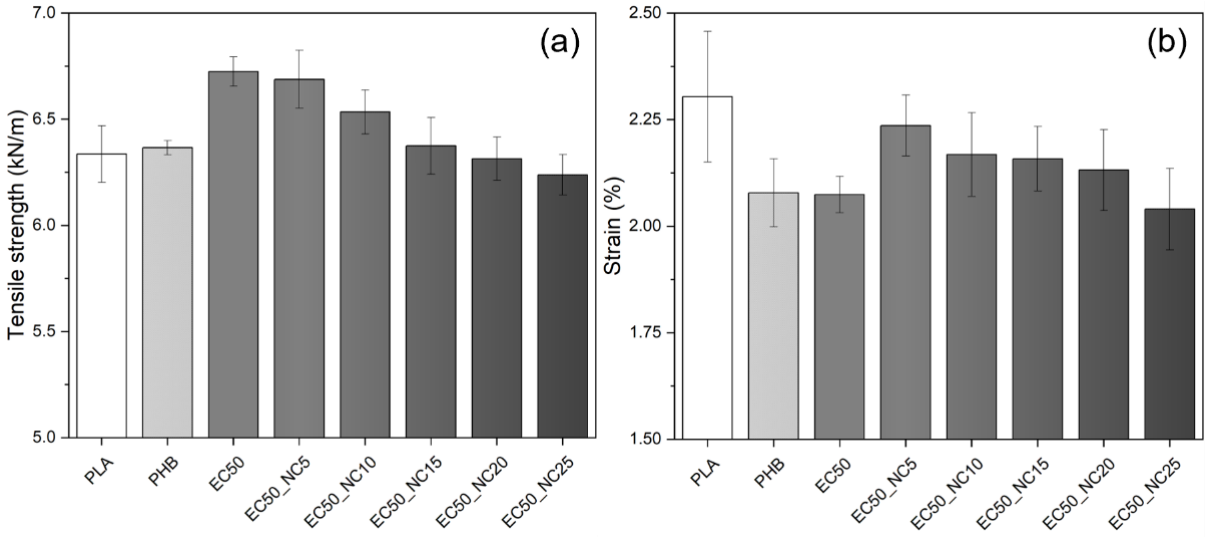

Fig. 12. Changes in the tensile strength (a) and strain (b) of the nanoclay reinforced PHB/EC blend-coated paper (coat weight: 18 g/m^2) depending on nanoclay content

CONCLUSIONS

1. When organically modified nanoclay, rendered hydrophobic by organic treatment, was applied as a filler in the polyhydroxybutyrate/ethyl cellulose (PHB/EC) blend coating formulation, up to 20% filler content exhibited uniform dispersion in the coating layer, showing excellent compatibility with the PHB/EC blend. Consequently, the barrier properties of the coated paper gradually improved in proportion to the nanoclay content.
2. However, when the filler content was increased to 25%, aggregation among nanoclay particles occurred, resulting in a diminishing enhancement of the barrier properties. The tensile strength of the PHB/EC blend coating film decreased with the addition of nanoclay, whereas the elongation at break increased, indicating a more ductile behavior.
3. Nevertheless, at a nanoclay level of 25%, elongation at break also decreased, compromising the mechanical properties of the coated paper.
4. The application of nanoclay as a filler in the PHB/EC blend shows promise for contributing to additional enhancements in the barrier and mechanical properties.

ACKNOWLEDGMENTS

This study was conducted with the support of the R&D Program for Forest Science Technology (Project No. 2023473B10-2325-EE02) provided by the Korea Forest Service (Korea Forestry Promotion Institute).

REFERENCES CITED

Agag, T., and Takeichi, T. (2000). "Polybenzoxazine–montmorillonite hybrid nanocomposites: Dynthesis and characterization," *Polymer* 41(19), 7083-7090. DOI: 10.1016/S0032-3861(00)00064-1

Ahmadi, P., Jahanban-Esfahlan, A., Ahmadi, A., Tabibiazar, M., and Mohammadifar, M. (2020). "Development of ethyl cellulose-based formulations: A perspective on the novel technical methods," *Food Rev. Int* 38(4), 685-732. DOI: 10.1080/87559129.2020.1741007

Aramvash, A., Akbari Shahabi, Z., Dashti Aghjeh, S., and Ghafari, M. D. (2015). "Statistical physical and nutrient optimization of bioplastic polyhydroxybutyrate production by *Cupriavidus necator*," *Int. J. Environ. Sci. Technol* 12(7), 2307-2316. DOI: 10.1007/s13762-015-0768-3

Bedian, L., Villalba-Rodríguez, A. M., Hernández-Vargas, G., Parra-Saldivar, R., and Iqbal, H. M. (2017). "Bio-based materials with novel characteristics for tissue engineering applications–a review," *Int. J. Biol. Macromol* 98, 837-846. DOI: 10.1016/j.ijbiomac.2017.02.048

Botana, A., Mollo, M., Eisenberg, P., and Sanchez, R. M. T. (2010). "Effect of modified montmorillonite on biodegradable PHB nanocomposites," *Appl. Clay Sci* 47(3-4), 263-270. DOI: 10.1016/j.clay.2009.11.001

Bugnicourt, E., Cinelli, P., Lazzeri, A., and Alvarez, V. (2014). "Polyhydroxyalkanoate (PHA): review of synthesis, characteristics, processing and potential applications in packaging," *Exp. Polym. Lett* 8, 791-808. DOI: 10.3144/expresspolymlett.2014.82

Chan, R. T. H., Garvey, C. J., Marcal, H., Russell, R. A., Holden, P. J., and Foster, L. J. R. (2011). "Manipulation of polyhydroxybutyrate properties through blending with ethyl-cellulose for a composite biomaterial," *Int. J. Polym. Sci.* DOI: 10.1155/2011/651549

Chen, J., Wu, D., and Pan, K. (2016). "Effects of ethyl cellulose on the crystallization and mechanical properties of poly (3-hydroxybutyrate)," *Int. J. Biol. Macromol* 88, 120-129. DOI: 10.1016/j.ijbiomac.2016.03.048

Cole, M., Lindeque, P., Halsband, C., and Galloway, T. S. (2011). "Microplastics as contaminants in the marine environment: A review," *Mar. Pollut. Bull* 62, 2588-2597. DOI: 10.1016/j.marpolbul.2011.09.025

Costa, M. M. E., Cabral-Albuquerque, E. C. M., Alves, T. L. M., Pinto, J. C., and Fialho, R. L. (2013). "Use of polyhydroxybutyrate and ethyl cellulose for coating of urea granules," *J. Agric. Food Chem* 61, 9984-9991. DOI: 10.1021/jf401185y

Cui, Y., Kumar, S., Kona, B. R., and van Houcke, D. (2015). "Gas barrier properties of polymer/clay nanocomposites," *RSC Advances* 5(78), 63669-63690. DOI: 10.1039/C5RA10333A

Cyras, V. P., Commisso, M. S., and Vazquez, A. (2009). "Biocomposites based on

renewable resource: acetylated and nonacetylated cellulose cardboard coated with polyhydroxybutyrate," *Polymer* 50(26), 6274-6280. DOI: 10.1016/j.polymer.2009.10.065

Cyras, V. P., Commisso, M. S., Mauri, A., and Vazquez, A. (2007). "Biodegradable double-layer films based on biological resources: Polyhydroxybutyrate and cellulose," *J. Appl. Polym. Sci.* 106(2), 749-756. DOI: 10.1002/app.26663

Fatyeyeva, K., Chappey, C., and Marais, S. (2017). "Biopolymer/clay nanocomposites as the high barrier packaging material: recent advances," *Food Packaging* 425-463. DOI: 10.1016/B978-0-12-804302-8.00013-3

Finelli, L., Scandola, M., and Sadocco, P. (1998). "Biodegradation of blends of bacterial poly (3-hydroxybutyrate) with ethyl cellulose in activated sludge and in enzymatic solution," *Mol. Chem. Phys* 199(4), 695-703. DOI: 10.1002/macp.1998.021990425

Gaikwad, K. K., and Ko, S. (2015). "Overview on polymer-nano clay composite paper coating for packaging application," *J. Mater. Sci. Eng.* 4(1), 151. DOI: 10.4172/2169-0022.1000151

Geyer, R., Jambeck, J. R., and Law, K. L. (2017). "Production, use, and fate of all plastics ever made," *Science Advances* 3(7), article e1700782. DOI: 10.1126/sciadv.1700782

Harding, K. G., Dennis, J. S., Von Blottnitz, H., and Harrison, S. T. L. (2007). "Environmental analysis of plastic production processes: comparing petroleum-based polypropylene and polyethylene with biologically-based poly-β-hydroxybutyric acid using life cycle analysis," *J. Biotechnol.* 130(1), 57-66. DOI: 10.1016/j.jbiotec.2007.02.012

Heinze, T., El Seoud, O. A., and Koschella, A. (2018). "Etherification of cellulose," in: *Cellulose Derivatives*, pp. 429-477. DOI: 10.1007/978-3-319-73168-1_6

Isa, M. R. M., Hassan, A., Nordin, N. A., Thirmizir, M. Z. A., and Ishak, Z. A. M. (2020). "Mechanical, rheological and thermal properties of montmorillonite-modified polyhydroxybutyrate composites," *High Perform. Polym* 32(2),192-200. DOI: 10.1177/0954008319899721

Khosravi-Darani, K., and Bucci, D. Z. (2015). "Application of poly (hydroxyalkanoate) in food packaging: Improvements by nanotechnology," *Chem. Biochem. Eng. Quart* 29(2), 275-285. DOI: 10.15255/CABEQ.2014.2260

Khwaldia, K., Arab-Tehrany, E., and Desobry, S. (2010). "Biopolymer coatings on paper packaging materials," *Comprehensive Reviews in Food Science and Food Safety* 9(1), 82-91. DOI: 10.1111/j.1541-4337.2009.00095.x

Ko, J. K. (2021). "Microbial synthesis of biodegradable polyhydroxyalkanoates (PHAs)," *Polym. Sci. Technol* 32(1), 4-7.

Koller, M., Salerno, A., Dias, M., Reiterer, A., and Braunegg, G. (2010). "Modern biotechnological polymer synthesis: A review," *Food Technol. Biotechnol* 48(3), 255-269.

Lee, S. S., Jung, K. S., and Yeo, J. K. (1987). "Toughening mechanism of plastics II. Fracture behavior of semicrystalline plastics," *Polymer* (Korea) 11(1), 2-20.

Li, X., Jiang, F., Ni, X., Yan, W., Fang, Y., Corke, H., and Xiao, M. "Preparation and characterization of konjac glucomannan and ethyl cellulose blend films," *Food Hydrocolloids* 44, 229-236. DOI: 10.1016/j.foodhyd.2014.09.027

Lim, D. G., Lee Y. J., Lee J. M., Kim J. H., Lee T. J., and Kim H. J. (2024). "Effect of polyhydroxybutyrate and ethyl cellulose for barrier coating of kraft paper," *BioResources* 19, 1618-1632. DOI: 10.15376/biores.19.1.1618-1632

Lim, D. G., Park, N. Y., Lee, Y. J., Yun, J. H., and Kim, H. J. (2021). "Characterization of the paper coated with polyhydroxybutyrate/ethyl cellulose blends," *J. Korea TAPPI* 53(4), 41-52. DOI: 10.7584/JKTAPPI.2021.08.53.4.41

Liu, Y., Ahmed, S., Sameen, D. E., Wang, Y., Lu, R., Dai, J., Li, S., and Qin, W. (2021). "A review of cellulose and its derivatives in biopolymer-based for food packaging application," *Trends Food Sci Technol* 112, 532-546. DOI: 10.1016/j.tifs.2021.04.016

Ministry of Environment, Comprehensive countermeasures for recycling waste management, (2018).

Motawie, A. M., Madany, M. M., El-Dakrory, A. Z., Osman, H. M., Ismail, E. A., Badr, M. M., El-Komy, D. A., and Abulyazied, D. E. (2014). "Physico-chemical characteristics of nano-organo bentonite prepared using different organo-modifiers," *Egypt. J. Petrol.* 23(3), 331-338. DOI: 10.1016/j.ejpe.2014.08.009

Official Journal of the European Union, L150, pp. 141-154 (2018).

Rastogi, V. K., and Samyn, P. (2020). "Compression molding of polyhydroxybutyrate nano-composite films as coating on paper substrates," *Mater. Proc.* 2(1), 31. DOI: 10.3390/CIWC2020-06797

Rastogi, V. K., and Samyn, P. (2017). "Synthesis of polyhydroxybutyrate particles with micro-nanosized structures and application as protective coating for packaging papers," *Nanomaterials* 7(1), article 5. DOI: 10.3390/nano7010005

Safari, S., and van de Ven, T. G. M. (2015). "Effect of crystallization conditions on the physical properties of a two-layer glassine paper/polyhydroxybutyrate structure," *J. Mater. Sci* 50(10), 3686-3696. DOI: 10.1007/s10853-015-8929-9

Seoane, I. T., Luzi, F., Puglia, D., Cyras, V. P., and Manfredi, L. B. (2018). "Enhancement of paperboard performance as packaging material by layering with plasticized polyhydroxybutyrate/nanocellulose coatings," *J. Appl. Polym. Sci* 135(48), 1-11. DOI: 10.1002/app.46872

Seoane, I. T., Manfredi, L. B., and Cyras, V.P. (2018). "Bilayer biocomposites based on coated cellulose paperboard with films of polyhydroxybutyrate/cellulose nanocrystals," *Cellulose* 25, 2419-2434. DOI: 10.1007/s10570-018-1729-z

Seoane, I. T., Manfredi, L. B., Cyras, V. P., Torre, L., Fortunati, E., and Puglia, D. (2017). "Effect of cellulose nanocrystals and bacterial cellulose on disintegrability in composting conditions of plasticized PHB nanocomposites," *Polymers* 9(11), article 561. DOI: 10.3390/polym9110561

Verlinden, R. A., Hill, D. J., Kenward, M. A., Williams, C. D., and Radecka, I. (2007). "Bacterial synthesis of biodegradable polyhydroxyalkanoates," *J. Appl. Microbiol.* 102(6), 1437-1449. DOI: 10.1111/j.1365-2672.2007.03335.x

Wang, S., Lydon, K. A., White, E. M., Grubbs III, J. B., Lipp, E. K., Locklin, J., and Jambeck, J. R. (2018). "Biodegradation of poly (3-hydroxybutyrate-co-3-hydroxyhexanoate) plastic under anaerobic sludge and aerobic seawater conditions: Gas evolution and microbial diversity," *Envir. Sci. Tech.* 52(10), 5700-5709. DOI: 10.1021/acs.est.7b06688

Zhang, L., Deng, X., and Huang, Z. (1997). "Miscibility, thermal behavior and morphological structure of poly(3-hydroxybutyrate) and ethyl cellulose binary blends," *Polymer* 38(21), 5379-5387. DOI: 10.1016/S0032-3861(97)84642-3

Article submitted: February 26, 2024; Peer review completed: March 23, 2024; Revised version received: Mary 17, 2024; Accepted: May 21, 2024; Published: May 31, 2024.
DOI: 10.15376/biores.19.3.4782-4799

APPENDIX

Supplementary Material

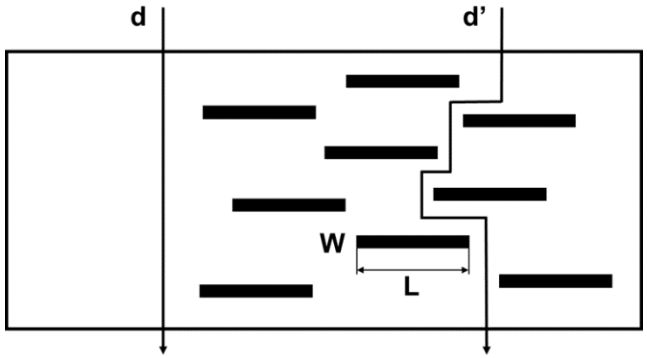

Fig. S1. The tortuous pathway in polymer/clay nanocomposites (inspired by Fatyeyeva *et al.* 2017)